Publishing House
AKAPIT

COMPUTER METHODS IN MATERIALS SCIENCE

Informatyka w Technologii Materiałów

Vol. 12, 2012, No. 3

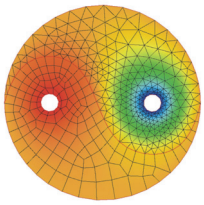

DETERMINATION OF THE CRITICAL PARAMETERS FOR THE ONSET OF DYNAMIC RECRYSTALLIZATION (DRX) IN ADVANCED ULTRA-HIGH STRENGTH STEELS (A-UHSS) MICROALLOYED WITH BORON

GERARDO ALTAMIRANO GUERRERO[1], IGNACIO MEJÍA GRANADOS[1,*], JOSÉ MARÍA CABRERA MARRERO[2, 3]

[1] Instituto de Investigaciones Metalúrgicas, Universidad Michoacana de San Nicolás de Hidalgo, Edificio "U", Ciudad Universitaria, 58066 – Morelia, Michoacán, México
[2] Departament de Ciència dels Materials i Enginyeria Metallúrgica, ETSEIB – Universitat Politècnica de Catalunya, Av. Diagonal 647, 08028 – Barcelona, Spain.
[3] Fundació CTM Centre Tecnològic, Av. de las Bases de Manresa, 1, 08240 – Manresa, Spain
**Corresponding author: imejia@umich.mx, i.mejia.granados@gmail.com*

Abstract

In this research work, the double differentiation mathematical method was used to identify more accurately the critical stress (σ_c) and critical strain (ε_c) associated with the onset of dynamic recrystallization (DRX), which is based on changes of the strain hardening rate ($\theta = \partial\sigma/\partial\varepsilon$) as a function of the flow stress (Poliak and Jonas method, simplified by Najafizadeh and Jonas). For this purpose, a low carbon advanced ultra-high strength steel (A-UHSS) microalloyed with different amounts of boron (14, 33, 82, 126 and 214 ppm) was deformed by uniaxial hot-compression tests at high temperatures ($950, 1000, 1050\ and\ 1100°C$) and constant true strain rates ($10^{-3}, 10^{-2} and\ 10^{-1}\ s^{-1}$). Results indicate that both σ_c and ε_c increase with decreasing deformation temperature and increasing strain rate. On the other hand, these critical parameters tend to decrease as boron content increases. Such a behavior is attributed to a solute drag effect by boron atoms on the austenitic grain boundaries and also to a solid solution softening effect.

Key words: advanced ultra-high strength steels; hot deformation; dynamic recrystallization; critical stress; critical strain; strain hardening rate

1. INTRODUCTION

In recent years, the automotive industry has promoted the development of new steels in order to reduce weight and built more efficient and safer cars. Advanced Ultra-High Strength Steels (A-UHSS) such as dual phase (DP), complex phase (CP), boron steels (BS) and martensitic steels (MART) have been developed for this purpose (Opbroek, 2009). These latest generation steels with multiphase microstructures, consisting of ferrite, martensite, bainite, and retained austenite are characterized by an excellent combination of high strength, good toughness and ductility. To reach these outstanding mechanical properties, alloying and microalloying elements such as C, Mn, Si, Nb, Ti, V, Zr and B are added to steel in combination with a suitable thermomechanical treatment (Meyer et al., 1985; Misra et al., 2001). As is well known, the microstructural control of metallic materials during hot forming operations is very important since it allows controlling the final microstructure

 ISSN 1641-8581

and, consequently the desired mechanical properties of alloys (Jonas, 1994).

Nowadays, one of the most important mechanisms for the microstructural control is dynamic recrystallization (DRX), which takes place during hot deformation of several metals and alloys. From laboratory simulations of metal forming, the occurrence of DRX is indicated by a well defined peak stress value in the experimental true stress–strain $(\sigma - \varepsilon)$ curves. However, it has been found (Luton & Sellars, 1969) that DRX actually starts at strain values lower than those corresponding to the peak stress (σ_p). This threshold strain is known as the critical strain(ε_c), and is linked with the minimum amount of stored energy induced by deformation needed to start the DRX (Poliak & Jonas, 1996). However, the critical stress value (σ_c) needed to detect the precise onset of DRX cannot be easily measured on the flow curves and for simplicity; some authors extrapolate this to σ_p (Le Bon et al., 1973). Due to the great influence of DRX on the microstructure and final mechanical properties of steels, several methods have been proposed to calculate the true σ_c for initiation of DRX on the basis of mathematical methods. It is possible to determine the ε_c by the method developed by Ryan and McQueen (1990) which defines the ε_c as the strain at which the experimental flow curve deviates from the idealized dynamic recovery (DRV) curve; it is based on differences in the strain hardening behavior associated with DRX and DRV. An alternative method and the most used to determine the critical conditions for the onset of DRX is that developed by Poliak and Jonas (1996, 2003a, 2003b) which eliminates the need for extrapolated flow stress data; the onset of DRX is identified by an inflection point in the strain hardening rate-stress $(\theta - \sigma)$ curve $(where\ \theta = d\sigma/d\varepsilon)$. These researchers have shown that this inflection point corresponds to the appearance of an additional thermodynamic degree of freedom in the system. This means that in addition to DRV an additional softening mechanism begins to operate. The additional mechanism can be phase transformation, twinning, or precipitate coarsening, but has been identified as DRX in this case. This method was later simplified by Najafizadeh and Jonas (2006). The most significant difference between this and the previous method is that a 3rd order polynomial equation was used to fit experimental $(\theta - \sigma)$ curve.

On the other hand, different factors such as the chemical composition of steel can significantly alter the critical conditions $(\sigma_c,\ \varepsilon_c)$ for DRX (Luton & Sellars, 1969; Sakai & Jonas, 1984; Sah et al., 1974), e.g., carbon is considered one of the interstitial elements that has more influence on the hot flow behavior of steel. Several researches (Wray, 1982; Wray, 1984; Xu et al., 1995**)** have reported that carbon produces a solid solution softening effect additional to that produced by DRX. Increasing the carbon content in the steel decreases the work hardening and the flow stress. Likewise, the apparent activation energy for hot deformation (Q_{def}) decreases with increasing the carbon content in the steel resulting in a faster onset of DRX (Serajzadeh & Taheri, 2003). Another element that has been found improves the hot flow behavior of steel in a similar or higher level than carbon is boron (Song et al., 2003; Lopez Chipres et al., 2007. Lopez Chipres et al., 2008; Mejía et al., 2011). However, the role played by boron atoms on the hot deformation of steels has not yet been well established. Lagerguist and Langnenberg (1972) indicated that because boron is a small atom it segregates readily to the grain boundaries reducing the grain boundary sliding so improving creep ductility. Hondros and Seah (1977) reported that the segregated boron on austenite grain boundaries changes the thermodynamic characteristics of these boundaries and this may have some effect on the softening behavior of austenite during hot working.

Nowadays, there is not relevant information about boron effect on the critical conditions for the onset and kinetics of DRX in advanced ultra-high strength steels (A-UHSS). In this research work, the simple method of Najafizadeh and Jonas (2006) was applied for determination of σ_c and ε_c to detect the precise onset of DRX. Consequently, the effect of boron additions and the deformation parameters (temperature and constant strain rate) on such critical conditions for the initiation of DRX in a low carbon advanced ultra-high strength steel (A-UHSS) under hot compression tests are also determined.

2. EXPERIMENTAL PROCEDURE

2.1. Materials and experimental route

The experimental low carbon Advanced Ultra-High Strength Steels (A-UHSS) were melted in the Foundry Laboratory of the Metallurgical Research Institute-UMSNH (México) using high purity raw materials in a 25 kg capacity induction furnace and cast into 70 mm × 70 mm cross section ingots.

Chemical compositions of the steels analyzed in this study are shown in table 1. The base composition is 0.15C-0.50Cu-1.31Cr-2.44Ni-0.22V (B0 steel). In order to study the individual effect of boron, the content thereof was varied in B1-B5 steels.

($10^{-3}, 10^{-2} and\ 10^{-1}\ s^{-1}$) and quenched in water immediately after strained. Two tantalum thin foils and boron nitride were used as lubricants to minimize friction effects and the subsequent barreling of the specimen. Because the total strain was only $\varepsilon = 0.8$, and according to previous result (Cabrera et al., 1999) no correction was made of the flow curves due to friction. As well, because the strain rates involved were not very large, adiabatic correction was not necessary (Cabrera et al., 1999).

Table 1. *Chemical composition of the experimental advanced ultra-high strength steels (A-UHSS) (wt. %).*

Steel	C	Mn	Si	S	P	Cu	Cr	Ni	V	Al	N	B
B0	0.15	0.40	0.42	0.02	0.013	0.52	1.31	2.44	0.22	0.0026	0.0091	0
B1	0.12	0.40	0.40	0.02	0.012	0.51	1.31	2.38	0.22	0.0040	0.0100	0.0014
B2	0.11	0.41	0.43	0.01	0.007	0.46	1.33	2.26	0.24	0.0048	0.0082	0.0033
B3	0.11	0.40	0.35	0.02	0.012	0.51	1.30	2.37	0.22	0.0030	0.0086	0.0082
B4	0.10	0.40	0.33	0.01	0.011	0.49	1.30	2.30	0.22	0.0036	0.0079	0.0126
B5	0.09	0.41	0.29	0.02	0.012	0.50	1.30	2.42	0.22	0.0031	0.0087	0.0214

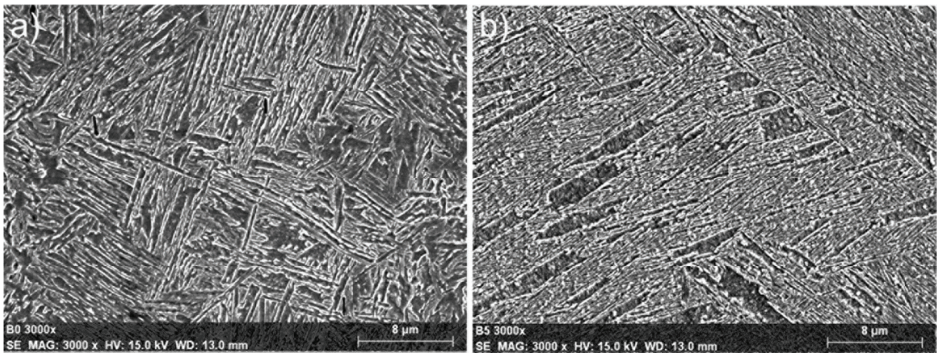

Fig. 1. *Microstructures of the present advanced ultra-high strength steels (AUHSS): a) B0 steel (0 ppm B) and b) B5 steel (214 ppm B).*

Uniaxial tensile tests revealed that in the as hot-rolled + quenched condition the ultimate tensile strength goes from 925 MPa for B0 steel to 1135 MPa for B5 steel with complex phases consisting mainly of bainite and martensite, as can be seen in figure 1.

Cylindrical specimens of 7 mm in diameter and 11 mm in length were machined from the as cast condition steels ingots. Isothermal hot compression tests were done at different temperatures and constant true strain rates using an *Instron* tensile testing machine equipped with a radiant cylindrical furnace. All tests were undertaken in an argon atmosphere in order to protect the molybdenum-based tools from oxidation as well as to prevent oxidation of the samples. First of all, the specimens were heated to 1100°C and held for 900 s to homogenize the microstructure and to obtain a similar initial grain size. Then specimens were cooled down to the test temperatures ($950, 1000, 1050\ and\ 1100°C$) and held again for 300 s. Specimens tested at 1100°C were strained directly after of the homogenization treatment. All specimens were strained until $\varepsilon = 0.8$ at different constant true strain rates

2.2. Mathematical method for determining the onset of DRX

The method developed by Poliak and Jonas (1996, 2003a, 2003b) and subsequently simplified by Najafizadeh and Jonas (2006) was used to identify the critical condition of stress and strain ($\sigma_c\ and\ \varepsilon_c$) associated with the real onset of DRX. First of all, the elastic portion of each experimental flow curve was removed and then these were fitted and smoothed to region beyond of peak stress, with a 9^{th} order polynomial. The smoothing eliminated the irregularities and fluctuations present in the experimental curves and in this way allowed the subsequent calculations. These experimental $\sigma - \varepsilon$ smoothed curves were then employed to calculate the value of the strain hardening rate by the differentiation of these, i.e. $\theta = d\sigma/d\varepsilon$. DRX causes a downward inflection in the $\theta - \sigma$ plot, leading to zero and negative strain hardening rates; according to the approach of Poliak and Jonas (1996, 2003a, 2003b) and Ryan and McQueen (1990) the point where the plot crosses the zero from above represent

the peak stress (σ_p) and the inflection point indicates the critical stress (σ_c) for the initiation of DRX. The method involves differentiating the experimental $\theta - \sigma$ curve**.** However, such differentiation usually does not exhibit clearly the inflection point and the exact onset of recrystallization is uncertain. According to Najafizadeh and Jonas (2006) this inflection point can be clearly detected by fitting a 3rd order polynomial equation to the experimental $\theta - \sigma$ curve up to the peak point as follows:

$$\theta = A\sigma^3 + B\sigma^2 + C\sigma\ D \qquad (1)$$

where *A, B, C,* and *D* are constants for a given set of deformation conditions. Differentiation of this equation with respect to σ results in:

$$\frac{d\theta}{d\sigma} = 3A\sigma^2 + 2B\sigma + C \qquad (2)$$

At critical stress for initiation of DRX, the second derivative becomes zero. Therefore,

$$\frac{d^2\theta}{d\sigma} = 0 \rightarrow 6A\sigma_c + 2B + 0 \rightarrow \sigma_c = \frac{-B}{3A} \qquad (3)$$

According to Poliak and Jonas (1996, 2003a, 2003b) the next step required to identify the critical stress (σ_c) is to plot the derivative of the 3rd order equation *versus* flow stress $(d\theta/d\sigma - \sigma)$ and the minimum points in these plots represent the σ_c. Once σ_c has been identified, the critical strain value (ε_c) can be found on the experimental true stress-strain data. Figure 2 schematically summarizes the steps for obtaining of the critical value for initiation of DRX by the application of this mathematical method. As mentioned above, the onset of DRX is not directly measurable on the experimental $\sigma - \varepsilon$ curves. Then, some authors suggest that the value of deformation needed to start the DRX is proportional to the peak strain (Le Bon et al., 1973). However, as corroborated in figure 2, σ_p and σ_c values are very different. σ_c value is significantly lower, which indicates that DRX starts well before the strain corresponding to σ_p.

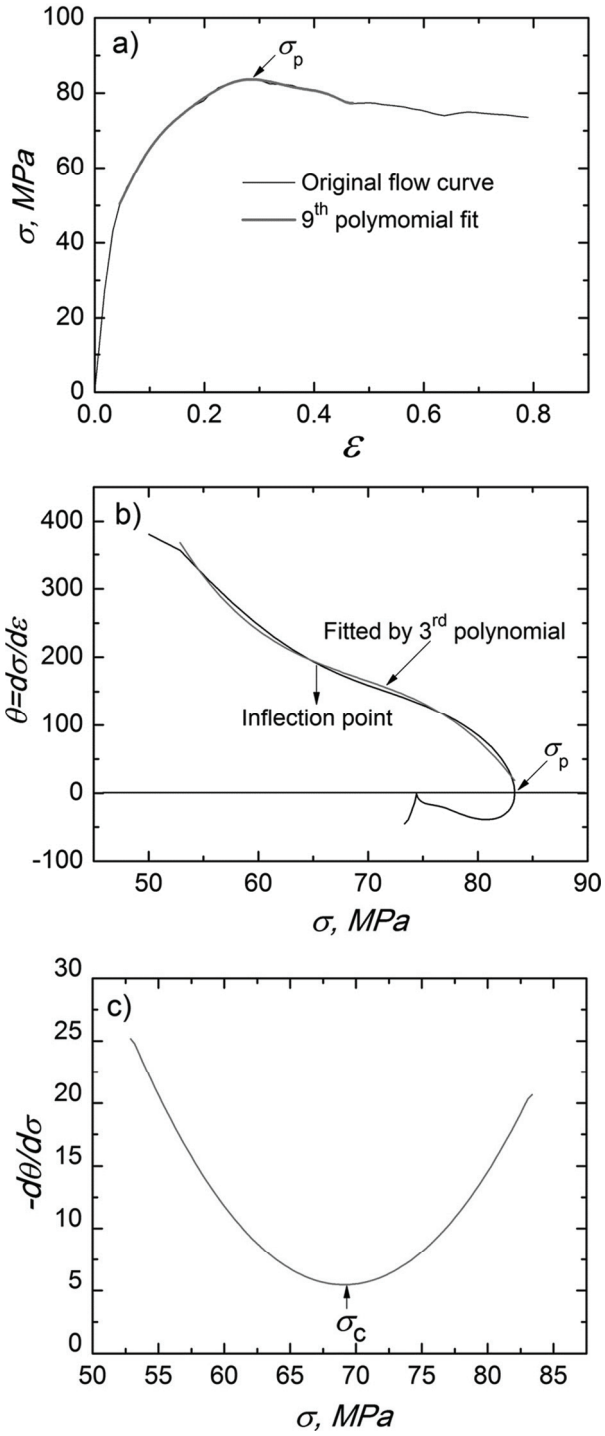

Fig. 2. *Method used for determination of the critical stress associated with the onset of DRX.*

3. RESULTS AND DISCUSSION

3.1. Hot flow curves

Examples of the flow stress–strain $(\sigma - \varepsilon)$ curves obtained from the hot compression tests are given in figure 3 for B0 and B5 steels. Similar results were recorded in the other steels. As expected, these hot flow curves show the typical behavior when DRX occurs (Roberts, 1982; Sakai & Jonas, 1984; Humphreys & Hatherly, 2004; López Chipres et al., 2008; Mejía et al., 2008; Mejía et al., 2011), i.e. after reaching a maximum stress value, a sharp drop to a steady-state stress level is observed. Likewise, all hot flow curves exhibited the classic dependence of σ_p and ε_p on temperature and strain rate, i.e., these parameters tend to increase as strain rate increases and temperature decreases. As is well known, the lower the temperature the softening processes are less active and, therefore, a greater stress

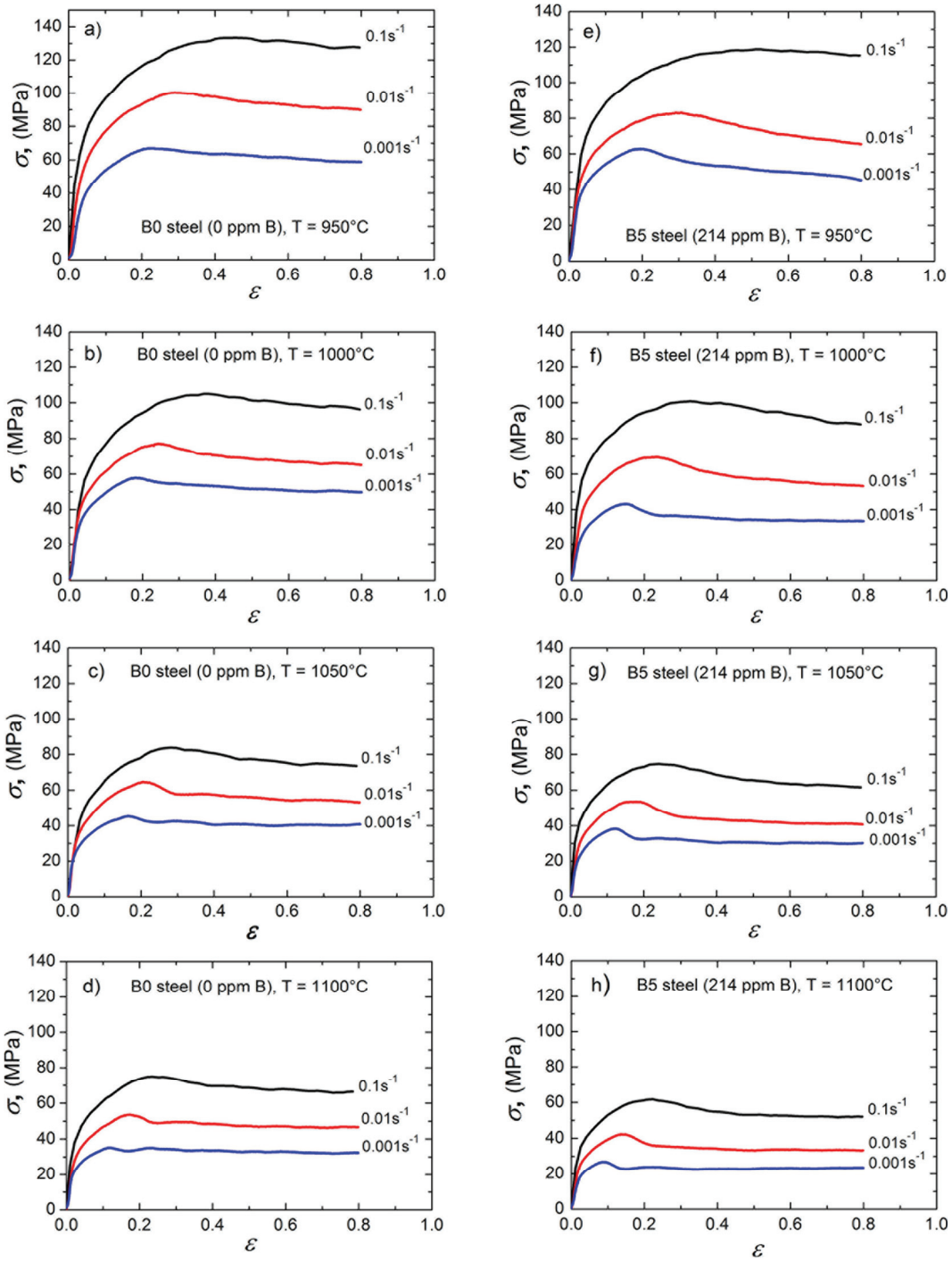

Fig. 3. *Hot flow curves for B0 and B5 steels as a function of the strain rate for all test temperatures (950, 1000, 1050, 1100°C).*

is required to deform the material. Similarly, the higher strain rate less time is available for nucleation and growth of new grains, i.e. for the occurrence of DRX. Therefore, as illustrated in figure 3, DRX preferably appears at strain rates of 0.01 and 0.001 s^{-1} and at relatively high temperatures (1000-1100 °C). Under these conditions Schulson et al., (1985) have reported that boron improves the mobility of grain boundary dislocations during hot deformation, which in turns facilitates the DRX. This reason would explain partially the present acceleration of the onset of DRX (diminution of σ_p and ε_p) at increasing boron content. These results also indicate that boron additions could promote a solid solution softening effect additional to the DRX itself, in a similar way to the role played by other interstitial alloying elements such as carbon in steels (Wray, 1982; Wray, 1984; Xu et al., 1995). This solid solution softening effect can be associated with diffusion and segregation of the boron atoms towards the austenitic grain boundaries where they occupy the vacancies generated by the applied deformation and

modify and reinforce the cohesion of austenitic grain boundaries; this fact would allow an easier plastic flow in the austenitic lattice (He et al., 1991; Song et al., 2003). Such behavior exhibited by the present A-UHSS microalloyed with boron at high temperatures is opposite to that shown at low temperatures, where increasing the boron content increases the hardness of steel (Wang & He, 2002).

tenite for iron-carbon alloys is improved by additions of interstitial alloying elements such as boron (Jahazi & Jonas, 2002). Finally, a slight delay of DRX kinetics at increasing boron content was detected in the flow curves. This effect was noted in the time spent in attaining the steady state stress once DRX has started. The delay of the DRX kinetics is usually associated to a solute drag effect (Saki

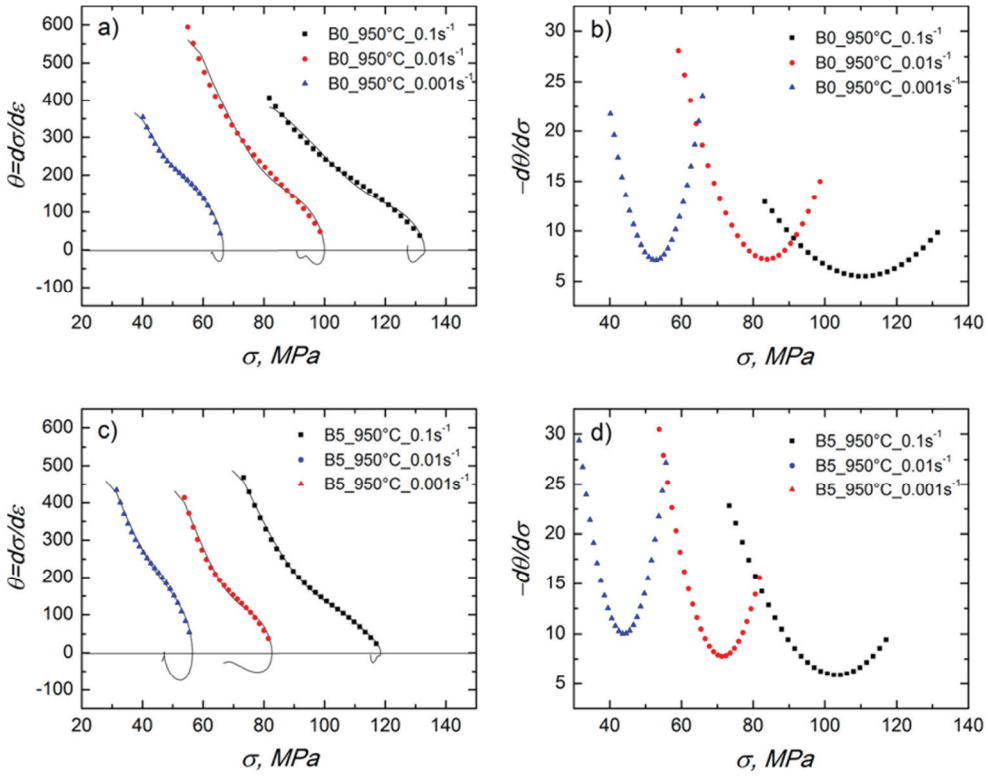

Fig. 4. *Strain hardening rate analyses for B0 and B5 steels at 950°C and 0.1, 0.01 and 0.001 s^{-1}.*

On the other hand, as is well known, the activation energy for hot deformation (Q_{def}) gives information about the difficulty of the atomic rearrangements involved in the rate-controlled mechanism, such as DRX (Medina & Hernandez, 1996). Also, the Q_{def} value depends on the steel grade and is very sensitive to small changes in the chemical composition (Sellars & McG Tegart, 1966). On this basis, the present authors (López Chipres et al., 2008; Mejía et al., 2008; Mejía et al., 2011) consider that boron can promote a diminution of Q_{def} and, therefore, accelerating the onset of DRX. Although Q_{def} has not been calculated for the present steels, the decrease of σ_p is a good indication that boron decreases the energy barrier for the hot deformation, i.e., accelerates the initiation of DRX. This positive effect on Q_{def} has already been confirmed by Kim et al., (2005) in interstitial free (IF) steels. Such behavior is possibly because the diffusion in the aus-

& Jonas, 1984) and it has already been reported by this research group in previous work (López Chipres et al., 2008).

3.2. Determination of critical stress (σ_c)

The experimental $\theta - \sigma$ curves and its corresponding 3rd order polynomial for B0 and B5 steels at 950°C and all strain rates used in this study are shown in figures 4a and 4c. As can be seen from these graphs, each curve consists primarily of three distinct segments. First, θ linearly decreases with the flow stress at low stresses. Second, the $\theta - \sigma$ curve gradually changes to a lower slope linear segment and third, the curve drops towards $\theta = 0$ to peak stress. As mentioned above, the inflection at critical stress indicates that DRX becomes operative (Poliak & Jonas, 1996, 2003a, 2003b; Ryan & McQueen, 1990). Points where the plot crosses zero from above represent σ_p, and points where it crosses zero from

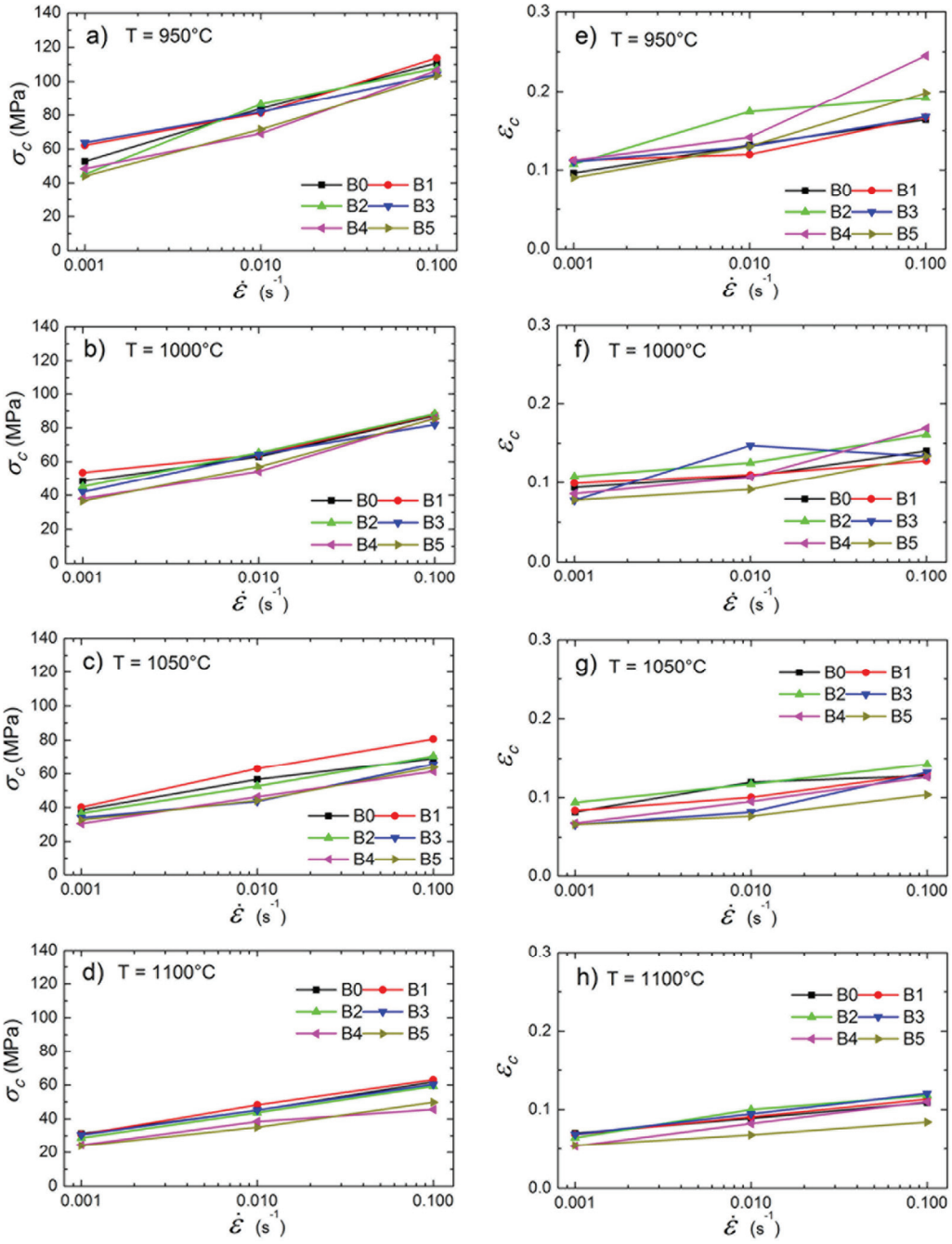

Fig. 5. *Dependence of the critical stress and critical strain on the strain rate at constant temperature.*

below represent stress valleys/minima. At this point, the σ_p value can be precisely measured as 67, 133 MPa for B0 steel at strain rates of 0.001, 0.01 and 0.1 s^{-1}, respectively (figure 4a), and 56, 83 and 119 MPa for B5 steel at equal condition of strain rate (figure 4c). Although the flow stress peaks in constant strain rate deformation are a good indication that DRX is well under way, they do not provide precise information about the onset of DRX. As already noted, the minimum points in the plots of the derivative of the 3rd order equation *versus* flow stress $(d\theta/d\sigma - \sigma)$ represent the exact σ_c associated with the onset of DRX. On this basis, σ_c values of 52, 83 and 110 MPa were recorded for B0 steel at strain rates of 0.001, 0.01 and 0.1s^{-1}, respectively, and 44, 71 and 110 MPa for B5 steel (see figures 4b and 4d). As can be seen in the graphs of figure 4, more stress is needed for the onset of DRX at increasing strain rate $(\dot{\varepsilon})$. On the other hand, the comparative analysis of the steel without boron content (B0) and the steel with the highest content (B5) indicates, that at all strain rates, B0 steel requires more stress and consequently a larger amount of deformation than the B5 steel for the onset of DRX. This method was used to

calculate the real critical values of stress and strain for initiation of DRX for all test conditions. All results are displayed in figure 5.

It is evident from figure 5 that boron additions produce softening during the hot deformation of the steel. In general, the steel with higher boron content (B5-214 ppm B) exhibit the greatest softening effect. The lowest values of σ_c and ε_c are observed in this steel, particularly at the highest test temperatures. Overall, the results of this study show that the higher the boron content the lower the stress for DRX onset. This softening mechanism can be related to the occurrence of an additional channel that facilitates formation of dislocations kinks at impurity centers (a decrease in kink energy with increasing solute content, facilitates the dislocation mobility) (Okazaki, 1996; Gornostyrev et al., 2005; Petukhov, 2007). Boron segregates towards austenitic grain boundary and promotes disordering and the consequent expected increase in grain boundary dislocations mobility, which in turn facilitates the onset of the DRX (Baker & Schulson, 1988). These phenomena are explained on the basis of the non-equilibrium segregation theory proposed by Aust et al. (1968), as an effect of mobile vacancy–solute atom complexes diffusing through a vacancy gradient towards vacancy sinks (this gradient can be generated by cooling and/or by plastic deformation). In this case, the grain boundary softening is probably caused by the presence of solute clusters resulting from the decomposition of vacancy–solute complexes near the boundary sink (Aust et al., 1965; Aust et al., 1968).

Additionally, this softening effect could be related to the dual nature of boron atoms in the austenite lattice and their environment. When these possess enough energy, they can move from their substitutional position to an interstitial one, experiencing this way an accelerated diffusion, which may accelerate the onset of DRX (Jahazi & Jonas, 2002). On the other hand, the relationship exhibited for the present steels between $\sigma_c - \dot{\varepsilon}$ and $\varepsilon_c - \dot{\varepsilon}$ (see figure 5) is similar to the shape observed in the absence of precipitation (no humps are observed); which suggests that the effect of boron on the kinetics of DRX is of the solute drag type (Mejía et al., 2008). The entire calculated DRX parameters in this study are listed in tables 2 and 3. As mentioned above, both σ_c and ε_c tend to increase as strain rate increases and temperature and boron content decreases. Furthermore, as can be seen in these tables, for the present advanced ultra-high strength steels microalloyed with boron the ε_c value associated with the onset of DRX is approximately $0.5\varepsilon_p$. The critical ratios of both σ_c/σ_p and $\varepsilon_c/\varepsilon_p$ remain fairly constant. The mean critical stress ratio is 0.82 and the mean critical strain ratio is 0.53. Similar values have been reported for other steels (Poliak & Jonas, 2003a, 2003b; Karjalainen et al., 1995; Siciliano & Jonas, 2000; Sun & Hawbolt, 1997; Shaban & Eghbali, 2010; Elwazri et al., 2004; Mirzadeh & Najafizadeh, 2010; Jafari & Najafizadeh, 2008; Mirzadeh et al., 2011; Kim et al., 2005). Finally, the dependence of critical strain on temperature and strain rate can be expressed as the following equation by Zener–Hollomon parameter:

$$\varepsilon_c = K_\varepsilon \cdot Z^{m_\varepsilon} \tag{4}$$

where K_ε and m_ε are material constants, Z is the Zener–Hollomon parameter, which is defined as:

$$Z = \dot{\varepsilon} \cdot exp\left(\frac{Q}{RT}\right) \tag{5}$$

where $\dot{\varepsilon}$ is the strain rate, Q is the activation energy for deformation, R is the universal gas constant and T is the absolute temperature. Q of 270 kJ mol^{-1} for lattice self diffusion of iron in austenite was employed. Employing this approach, ε_c theoretical relationships were determined from experimental data and fitted with equation (4) using the least-squares method, as shown in figure 6. As can be seen in this figure, there is a linear relationship between ε_c and Z. ε_c tends to increase as Z increases, i.e. as strain rate increases and temperature decreases. The resulting equations for ε_c of each analyzed steel are also indicated in the graph of figure 6.

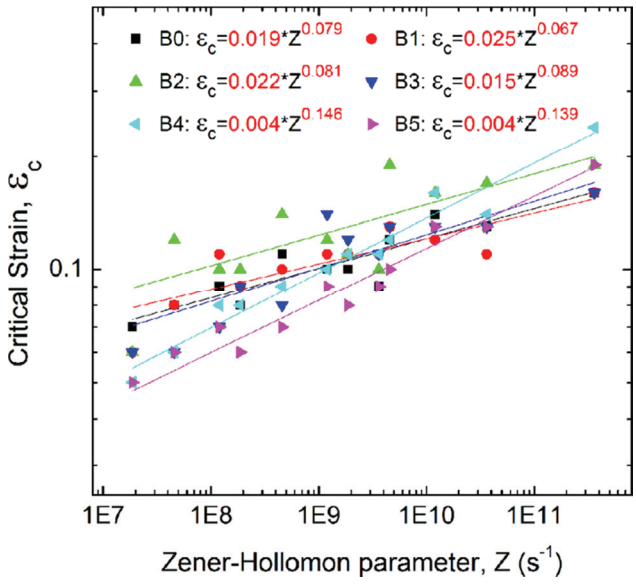

Fig. 6. *Dependence of the critical strain for the initiation of DRX on Zener–Hollomon parameter (Z) for each analyzed steel.*

Table 2. *Peak stress* (σ_p) *and critical stress* (σ_c) *values calculated for all test conditions.*

Steel	$\dot{\varepsilon} = 0.001s^{-1}$				$\dot{\varepsilon} = 0.01s^{-1}$			$\dot{\varepsilon} = 0.1s^{-1}$		
	T, °C	σ_p	σ_c	σ_c/σ_p	σ_p	σ_c	σ_c/σ_p	σ_p	σ_c	σ_c/σ_p
B0	950	67	53	0.79	100	84	0.84	133	111	0.83
	1000	58	48	0.82	77	62	0.80	105	87	0.82
	1050	45	39	0.86	65	57	0.87	83	70	0.84
	1100	35	31	0.88	54	45	0.83	75	62	0.82
B1	950	74	62	0.83	100	81	0.81	134	113	0.84
	1000	63	53	0.84	78	64	0.82	109	87	0.79
	1050	47	40	0.85	71	63	0.88	96	80	0.83
	1100	36	31	0.86	58	48	0.82	76	63	0.82
B2	950	70	45	0.64	100	86	0.86	131	107	0.81
	1000	54	45	0.83	79	65	0.82	107	88	0.82
	1050	43	37	0.86	63	53	0.84	86	71	0.82
	1100	34	28	0.82	53	44	0.83	73	59	0.80
B3	950	76	64	0.84	97	81	0.83	124	104	0.83
	1000	50	41	0.82	72	64	0.88	100	81	0.81
	1050	40	34	0.85	55	44	0.8	80	66	0.82
	1100	36	31	0.86	51	45	0.88	69	60	0.86
B4	950	57	48	0.84	81	69	0.85	116	106	0.91
	1000	46	38	0.82	65	54	0.83	98	86	0.87
	1050	36	30	0.83	56	46	0.82	75	61	0.81
	1100	30	24	0.80	48	38	0.79	65	46	0.70
B5	950	56	44	0.78	83	71	0.85	119	103	0.86
	1000	43	36	0.83	70	56	0.80	101	85	0.84
	1050	38	33	0.86	54	44	0.81	75	64	0.85
	1100	27	24	0.88	42	35	0.83	62	50	0.80

Table 3. *Peak strain* (ε_p) *and critical strain* (ε_c) *values calculated for all test conditions.*

Steel	$\dot{\varepsilon} = 0.001s^{-1}$				$\dot{\varepsilon} = 0.01s^{-1}$			$\dot{\varepsilon} = 0.1s^{-1}$		
	T, °C	ε_p	ε_c	$\varepsilon_c/\varepsilon_p$	ε_p	ε_c	$\varepsilon_c/\varepsilon_p$	ε_p	ε_c	$\varepsilon_c/\varepsilon_p$
B0	950	0.23	0.09	0.39	0.29	0.13	0.44	0.45	0.16	0.35
	1000	0.18	0.09	0.5	0.24	0.10	0.41	0.38	0.14	0.36
	1050	0.16	0.08	0.5	0.20	0.11	0.55	0.27	0.12	0.44
	1100	0.12	0.07	0.58	0.17	0.08	0.47	0.23	0.10	0.43
B1	950	0.22	0.11	0.5	0.27	0.11	0.40	0.44	0.16	0.36
	1000	0.19	0.09	0.47	0.21	0.11	0.52	0.35	0.12	0.34
	1050	0.16	0.08	0.5	0.21	0.10	0.47	0.29	0.13	0.44
	1100	0.13	0.06	0.46	0.19	0.09	0.47	0.24	0.11	0.45
B2	950	0.24	0.10	0.41	0.32	0.17	0.53	0.49	0.19	0.38
	1000	0.20	0.10	0.5	0.27	0.12	0.44	0.36	0.16	0.44
	1050	0.16	0.12	0.75	0.21	0.14	0.66	0.31	0.19	0.61
	1100	0.12	0.06	0.5	0.20	0.10	0.5	0.26	0.11	0.42
B3	950	0.22	0.11	0.5	0.32	0.13	0.40	0.49	0.16	0.32
	1000	0.15	0.07	0.46	0.23	0.14	0.60	0.34	0.13	0.38
	1050	0.12	0.06	0.5	0.18	0.08	0.44	0.29	0.13	0.44
	1100	0.12	0.06	0.5	0.16	0.09	0.56	0.21	0.12	0.57
B4	950	0.21	0.11	0.52	0.31	0.14	0.45	0.48	0.24	0.5
	1000	0.16	0.08	0.5	0.22	0.10	0.45	0.43	0.16	0.37
	1050	0.12	0.06	0.5	0.18	0.09	0.5	0.27	0.12	0.44
	1100	0.10	0.05	0.5	0.17	0.08	0.47	0.25	0.11	0.44
B5	950	0.19	0.09	0.47	0.30	0.13	0.43	0.52	0.19	0.36
	1000	0.15	0.07	0.46	0.23	0.09	0.39	0.32	0.13	0.40
	1050	0.11	0.06	0.54	0.17	0.07	0.41	0.24	0.10	0.41
	1100	0.09	0.05	0.55	0.13	0.06	0.46	0.22	0.08	0.36

4. CONCLUSIONS

1. From the experimental stress-strain curves, the double differentiation method provided precise results to determinate the critical conditions for the initiation of DRX.
2. A numerical approach on the dependence of the critical strain as a function of temperature and strain rate was determined for each studied steel.
3. In general, the σ_c and ε_c values tend to decrease as boron content increases, which indicates that boron additions generate a solid solution softening effect. The steel with 214 ppm of boron content exhibited the greatest softening effect.
4. The mean critical ratios of σ_c/σ_p and $\varepsilon_c/\varepsilon_p$ for the present advanced ultra-high strength steels microalloyed with boron were 0.82 and 0.53, respectively. These ratios are consistent with values reported for other steels, particularly C–Mn steels, microalloyed steels, high carbon and stainless steels.

REFERENCES

Aust, K.T., Hanneman, R.E., Niessssen, P., Westbrook, J.H., 1968, Solute-Induced Hardening near Grain Boundaries in Zone-Refined Metals, *Acta Metall.*, 16, 291-302.

Aust, K.T., Westbrook, J.H., in: Cotterill, R.M.J., Doyama, M., Jackson, J.J., Meshii, M., 1965, *Lattice Defects in Quenched Metals*, Academic Press, New York, 771-776.

Baker, I. Schulson, E.M., 1988, The Effect of Boron on the Chemistry of Grain Boundaries in Stoichiometric Ni3Al, *Philosophical Magazine*, 57, 379-385.

Cabrera, J.M., Prado, J.M., Barrón, M.A., 1999, An Inverse analysis of the Hot Uniaxial Compression test by means of the Finite Element Method, *Steel Res*., 70, 59-66.

Elwazri, A.M., Wanjara, P., Yue, S., 2004, Dynamic Recrystallization of Austenite in Microalloyed High Carbon Steels, *Mater. Sci. Technol.*, 20, 1469-1473.

Gornostyrev, Y.N., Katsnelson, M.I., Stroev, A.Y., Trefilov, A.V., 2005, Impurity-kink interaction in the two-dimensional Frenkel-Kontorova model, *Phys. Rev. B: Condens. Matter*, 71, 094105, 1-7.

He, X.L., Djahazi, M., Jonas, J.J., Jackman, J., 1991, The Non-equilibrium of Boron During the Recrystallization of Nb-treated HSLA Steels, *Acta Metall. Mater.,* **39**, 2295-2308.

Hondros, E.D., Seah, M.P., 1977, Segregation in Interfaces, *Review. Int. Met. Rev.*, 222, 262-301.

Humphreys, F.J., Hatherly, M., 2004, *Recrystallization and Related Annealing Phenomena*, Second ed., Elsevier Science, New York.

Jafari, M., Najafizadeh, A., 2008, Comparison between the Methods of Determining the Critical Stress for Initiation of Dynamic Recrystallization in 316 Stainless Steel, *J. Mater. Sci. Technol.*, 24, 840-844.

Jahazi, M., Jonas, J.J., 2002, The Non-equilibrium Segregation of Boron on Original and Moving Austenite Grain Boundaries, *Mater. Sci. Eng. A*, 335, 49-61.

Jonas, J.J., 1994, Dynamic Recrystallization–Cientific Curiosity or Industrial Tool?, *Mater. Sci. Eng. A*, 184, 155-165.

Karjalainen, L.P., Maccagno, T.M., Jonas, J.J., 1995, Softening and Flow-Stress Behavior of Nb Microalloyed Steels During Hot-Rolling Simulation, *ISIJ Int.*, 35, 1523-1531.

Kim, S.I., Choi, S.H., Lee, Y., 2005, Influence of Phosphorous and Boron on Dynamic Recrystallization and Microstructures of Hot-Rolled Interstitial Free Steel, *Mater. Sci. Eng. A*, 406, 125-133.

Lagerquist, M., Lagneborg, R., 1972, The Influence of Boron on the Creep Properties of Austenitic Stainless Steel, *Scand. J. Metall.*, 1, 81-89.

Le Bon, A., Rofes-Vernis, J., Rossard, C., 1973, Recrystallization and precipitation induced by high temperature deformation–Case of a weldable construction steel containing niobium, *Mem. Sci. Rev. Met.,* **70**, 577-588.

López Chipres, E., Mejía, I., Maldonado, C., Bedolla Jacuinde, A., Cabrera, J.M., 2007, Hot Ductility Behavior of Boron Microalloyed Steels, *Mater. Sci. Eng. A*, 460-461, 464-470.

López Chipres, E., Mejía, I., Maldonado, C., Bedolla Jacuinde, A. El-Wahabi, M., Cabrera, J.M., 2008, Hot Flow Behavior of Boron Microalloyed Steels, *Mater. Sci. Eng. A*, 480, 49-55.

Luton, M.J., Sellars, C.M., 1969, Dynamic Recrystallization in Nickel and Nickel-Iron Alloys during High Temperature Deformation, *Acta Metallurgica*, 17, 1033-1043.

Medina, S.F., Hernández, C.A., 1996, General Expression of the Zener-Hollomon Parameter as a Function of the Chemical Composition of Low Alloy and Microalloyed Steels, *Acta Mater.*, 44, 137-148.

Mejía, I., López Chipres, E., Maldonado, C., Bedolla Jacuinde, A., Cabrera., J.M., 2008, Modeling of the Hot Deformation Behavior of Boron Microalloyed Steels Under Uniaxial Hot Compression Conditions, *Int. J. Mater. Res. (formerly Z. Metallkd.)*, 99, 1336-1345.

Mejía, I., Maldonado, C., Bedolla Jacuinde, A., Cabrera., J.M., 2011, Determination of the Critical Conditions for the Initiation of Dynamic Recrystallization in Boron Microalloyed Steels, *Mater. Sci. Eng. A*, 528, 4133-4140.

Meyer, L., Strasburger, C., Schneider, C., 1985, Effect and Present Application of the Microalloying Elements Nb, V, Ti, Zr and B in HSLA Steels, *Proc. of HSLA'85*, Beijing, China, ASM-International, 29-39,

Mirzadeh, H., Najafizadeh, A., 2010, Prediction of the Critical Conditions for Initiation of Dynamic Recrystallization, *Mater. Des*., 31, 1174-1179.

Mirzadeh, H., Cabrera, J.M., Prado, J.M., Najafizadeh, A., 2011, Hot Deformation Behavior of a Medium Carbon Microalloyed Steel, *Mater. Sci. Eng. A*, 528, 3876-3882.

Misra, R.D.K., Weatherly, G.C., Hartmann, J.E., Boucek, A.J., 2001, Ultrahigh Strength Hot Rolled Microalloyed Steels: Microstructural Aspects of Development, *Mater. Sci. Technol.*, 17, 1119-1129.

Najafizadeh, A., Jonas, J.J., 2006, Predicting the Critical Stress for Initiation of Dynamic Recrystallization, *ISIJ Int.*, 46, 1679-1684.

Okazaki, K., 1996, Solid-Solution Hardening and Softening in Binary Iron-Alloys, *J. Mater. Sci.*, 31, 1087-1099.

Opbroek, E.G., 2009, International Iron & Steel Institute, Committee on Automotive Applications, *Advanced High Strength Steel Application Guidelines*, Brussels.

Poliak, E.I., Jonas, J.J., 1996, A One-Parameter Approach to Determining the Critical Conditions for the Initiation of Dynamic Recrystallization, *Acta Mater.*, 44, 127-136.

Poliak, E.I., Jonas, J.J., 2003a, Initiation of Dynamic Recrystallization in Constant Strain Rate Hot Deformation, *ISIJ Int.*, 43, 684-691.

Poliak, E.I., Jonas, J.J., 2003b, Critical Strain for Dynamic Recrystallization in Variable Strain Rate Hot Deformation, *ISIJ Int.*, 43, 692-700.

Petukhov, B.V., 2007, Effect of Solid-Solution Softening of Crystalline Materials: Review, *Crystallography Reports,* 52, 112-122.

Roberts, W., 1982, in: Krauss, G. (ed.), *Deformation, Processing and Structure*, ASM, Metals Park, OH., 109-184.

Ryan, N.D., McQueen, H.J., 1990, Dynamic Softening Mechanisms in 304 Austenitic Stainless Steel, *Can. Metall.*, Q 29, 147-162.

Sah, J.P., Richardson, G.J., Sellars, C.M., 1974, Grain-Size Effects During Dynamic Recrystallization of Nickel, *Met. Sci.*, 8, 325-331.

Sakai, T., Jonas, J.J., 1984, Dynamic Recrystallization: Mechanical and Microstructural Considerations, *Acta Metallurgica*, 32, 189-209.

Schulson, E.M., Weihs, T.P., Viens, D.V., Baker, I., 1985, The effect of Grain size on the Yield Strength of Ni_3Al, *Acta Metallurgica*. 33, 1587-1591.

Sellars, C.M., McG Tegart, W.J., 1966, La Relation Entre la Résistence et la Structure Dans la Déformation a Chaud, *Mem. Sci. Rev. Met.*, 63 (9), 731-746.

Serajzadeh, S., Taheri, A.K., 2003, An Investigation into the Effect of Carbon on the Kinetics of Dynamic Restoration and Flow Behavior of Carbon Steels, *Mechanics of Materials*, 35, 653-660.

Shaban, M., Eghbali, B., 2010, Determination of Critical Conditions for Dynamic Recrystallization of a Microalloyed Steel, *Mater. Sci. Eng. A*, 527, 4320-4325.

Siciliano Jr, F., Jonas, J.J., 2000, Mathematical Modeling of the Hot Strip Rolling of Microalloyed Nb, Multiply-Alloyed Cr-Mo, and Plain C-Mn Steels, *Metall. Mater. Trans. A*, 31, 511-530.

Song, S.H., Guo, A.M., Shen, D.D., Yuan, Z.X., Liu, J., Xu, T.D., 2003, Effect of Boron on the Hot Ductility of 2.25Cr1Mo Steel, *Mater. Sci. Eng. A*, 360, 96-100.

Sun, W.P., Hawbolt, E.B., 1997, Comparison between Static and Metadynamic Recrystallization–An Application to the Hot-Rolling of Steels, *ISIJ Int.*, 37, 1000-1009.

Xu, Z., Zhang, G-R., Sakai, T., 1995, Effect of Carbon Content on Static Restoration of Hot Worked Plain Carbon Steels, *ISIJ Int.*, 35, 210-216.

Wang, X.M., He., X.L., 2002, Effect on Boron Addition on Structure and Properties of Low Carbon Bainitic Steels, *ISIJ Int.*, 42, 38-46.

Wray, P.J., 1982, Effect of Carbon Content on the Plastic Flow of Plain Carbon Steels at Elevated Temperatures, *Metall. Mater. Trans. A*, 13, 125-134.

Wray, P.J., 1984, Effect of Composition and Initial Grain Size on the Dynamic Recrystallization of Austenite in Plain Carbon Steels, *Metall. Mater. Trans. A*, 15, 2009-2019.

WYZNACZANIE KRYTYCZNYCH PARAMETRÓW DLA ROZPOCZĘCIA REKRYSTALIZACJI DYNAMICZNEJ (DRX) I ZAAWANSOWANYCH STALACH O PODWYŻSZONEJ WYTRZYMAŁOŚCI Z DODATKIEM BORU

Streszczenie

Matematyczna metoda podwójnego różniczkowania została zastosowana dla dokładniejszej identyfikacji krytycznego naprężenia σ_c i krytycznego odkształcenia ε_c związanego z rozpoczęciem rekrystalizacji dynamicznej (DRX). Te dwa parametry są związane z prędkością umocnienia $\theta = \partial\sigma/\partial\varepsilon$ przedstawianą jako funkcja naprężenia uplastyczniającego (metoda Poliaka i Jonasa, uproszczona przez Najafizadeha i Jonasa). W tym celu niskowęglową stal o wysokiej wytrzymałości (ang. advanced ultra-high strength steel - AUHSS) wzbogacono różnymi zawartościami boru (0, 14, 33, 82, 126 i 214 ppm). Tą stal poddano odkształceniom plastycznym w wysokich temperaturach (950, 1000, 1050 i 1100^{o}C przy stałych prędkościach odkształcenia (10^{-3}, 10^{-2} i 10^{-1} s^{-1}). Otrzymane wyniki wykazały, że zarówno σ_c jak i ε_c rośnie wraz z obniżeniem się temperatury odkształcenia i wzrostem prędkości odkształcenia. Z drugiej strony, te krytyczne parametry zmniejszają się gdy wzrasta zawartość boru w stali. Jako przyczynę takiego zachowania uznano wpływ atomów boru w roztworze na granice ziaren austenitu a także wpływ mięknięcia roztworowego.

Received: July 31, 2012
Received in a revised form: December 12, 2012
Accepted: December 14, 2012